PROTEINS: Structure, Function, and Genetics 12:10–23 (1992)

RESEARCH ARTICLES

Functional Implications of Interleukin-1β Based on the Three-Dimensional Structure

B. Veerapandian,[1] Gary L. Gilliland,[1] Reetta Raag,[1] Anders L. Svensson,[1] Yoshihiro Masui,[2] Yoshikatsu Hirai,[2] and Thomas L. Poulos[1]

[1]Center for Advanced Research in Biotechnology, Maryland Biotechnology Institute, University of Maryland and National Institute of Standards and Technology, Rockville, Maryland 20850; and [2]Otsuka Pharmaceuticals, Tokushima 771-01, Japan

ABSTRACT **The molecular structure of interleukin-1β, a hormone-like cytokine with roles in several disease processes, has been determined at 2.0 Å resolution and refined to a crystallographic *R*-factor of 0.19. The framework of this molecule consists of 12 antiparallel β-strands exhibiting pseudo-3-fold symmetry. Six of the strands make up a β-barrel with polar residues concentrated at either end. Analysis of the three-dimensional structure, together with results from site-directed mutagenesis and biochemical and immunological studies, suggest that the core of the β-barrel plays an important functional role. A large patch of charged residues on one end of the barrel is proposed as the binding surface with which IL-1 interacts with its receptor.**

Key words: crystallography, molecular isomorphous replacement, molecular dynamics, refinement, interleukin, site-directed mutagenesis, receptor-binding surface, epitope

INTRODUCTION

Interleukin-1 (IL-1) belongs to the cytokine family of cellular mediators. These hormone-like proteins are produced primarily by activated mononuclear phagocytes in response to infection and injury.[1,2] IL-1 is also synthesized by a wide variety of cells including lymphocytes, vascular cells (smooth muscle cells, endothelial cells), skin cells (keratinocytes, langerhans cells), brain cells, and synovial fibroblasts. Transcription for IL-1 can be initiated in monocytes by cellular adherence to foreign surfaces. The cellular response to IL-1 varies among target cells, inducing the production of lymphokines such as interleukin-2, in interleukin-4, interleukin-6, B-cell differentiation factor, and colony-stimulating factor. Other responses include the production of prostaglandins and the proliferation of fibroblasts (for a detailed review see refs. 2,3,4). IL-1's presence in the synovial fluid of patients with arthritis suggests that IL-1 plays an important role in promoting chronic inflammation in joints.[5]

Two distinct species of IL-1 have been characterized, designated as interleukin-1α (IL-1α) and interleukin-1β (IL-1β).[6,7] Most of the membrane-associated IL-1 is of the α form whereas the β form is secreted into the extracellular fluid. Both these proteins are expressed as 31-kDa precursors which are processed by endoproteases[8–11] to give 17.5-kDa mature proteins. IL-1α is active as a precursor, whereas IL-1β is active only when processed.[12] They both bind to the same membrane receptor proteins.[13–16]

Extensive reviews on IL-1[3,17] have not revealed its functional characteristics. In order to understand how IL-1 interacts with its receptor, the three-dimensional structure determination of recombinant human interleukin-1β (IL-1β) has been carried out. The protein was first crystallized in our laboratory.[18] Simultaneous with our structure determination, other structural studies have also been reported.[19–22] In this paper we use our refined 2 Å structure together with a wealth of published biochemical and mutagenesis data to identify the regions of IL-1β which are responsible for receptor recognition, and to formulate a hypothesis for its mode of action.

EXPERIMENTAL PROCEDURES

Crystallisation and Data Collection

Purified recombinant human IL-1β was supplied by Otsuka Pharmaceuticals, Japan. Crystals were grown by vapor diffusion using the hanging drop technique as described in ref. 18. These crystals are tetragonal with $a = b = 55.14(2)$ Å and $c = 76.66$ (4) Å

Received February 7, 1991; accepted April 12, 1991.

Address reprint requests to Dr. B. Veerapandian, Center for Advanced Research in Biotechnology, 9600 Gudelsky Drive, Rockville, MD 20850.

Dr. Thomas L. Poulos is also affiliated with the Department of Chemistry, University of Maryland, Rockville, MD 20850.

and belong to the space group $P4_3$. Diffraction data were collected using a Siemen's electronic area detector and a Rigaku RU200 rotating anode X-ray generator operating at 3.2 kW, equipped with a graphite monochromator. The chamber was set at $2\theta = 20°$ and crystal to chamber distance was kept at 10 cm. Native data set was collected to a resolution of 2.0 Å with a total of 25,706 observations, scaled to give an R_{merge} of 0.05, where

$$R_{merge} = \frac{\Sigma|I_i - \langle I \rangle|}{|I_i|}$$

Of the available 14,207 unique reflections, 11,013 having $I > 2\sigma(I)$ were used for the rest of the analysis and refinement. Reduction of these data to integrated intensities was carried out using the XENGEN software package.[23]

TABLE Ia. Summary of Heavy Atom Compounds Tested*

Reagent	Scaling R between derivative and parent (%)
CH_3HgCl	23.1
UO_2SO_4	9.2
$UO_2CH_3CO_2$	8.7
$(NH_4)2RuCl_6$	9.6
$(Ir(NH_3)_5Cl)Cl_2$	10.6
TbCl	8.5
$NdNO_3$	14.9
$SmCH_3CO_2$	10.1
TmCl	8.6
$Au(CN)_4$	20.5
$Pt(CN)_4$	**21.7**
$Hg(CN)_4$	**28.8**
$Hg(CN)_4$ C8A mutant	**21.9**
Iodine	12.9
CH_3HgCl_2	20.4
UO_2NO_3	8.2

*The three derivatives (platinum and two mercury highlighted in bold print) were found to be the best derivatives and were selected for further MIR work. Heavy atom positions were located using difference Patterson and cross-difference Fouriers. Positional parameters (x,y,z, occupancy, and temperature factors) were refined and MIR phases calculated. A summary of the MIR refinement and statistics is given in Table Ib.

Structure Solution

Of the 16 derivative data sets collected (Table I), only three were used in the structure solution. All the derivative data sets extended to a resolution of 3 Å. Difference Patterson maps of mercurial and a few other derivatives showed one major binding site, later identified with Cys-8. Interpretation of the single isomorphous map arising from this site was difficult, even though some of the molecule's secondary structural features could be identified. Since IL-1β contains two cysteines, site-directed mutagenesis was used to change Cys-8 to alanine. Mutant protein was prepared with Cys-8 changed to Ala-8 without altering Cys-71 and used to make heavy atom derivatives. Mutant derivative crystals were found to be isomorphous with those of wild-type protein. Difference Patterson analysis revealed another heavy atom site, later confirmed to be close to Cys-71.

Scaling, merging and MIR steps were carried out using the PROTEIN[24] software package. The x and y coordinates of the sites were determined from the Harker section at $w = 1/2$. Since the space group is of the enantiomeric pair, $P4_3$ or $P4_1$, wherein the origin is not defined, the z coordinate of the first site was initially fixed at 0.1. The centric data alone were used in order to refine the spatial coordinates, occupancies, isotropic temperature factors, and overall scale factors of these sites. Difference Fourier and cross difference Fourier maps confirmed the major sites and a few minor sites were also identified (Table I). Using these sites native MIR phases were calculated to a resolution of 3.0 Å and the electron density map showed well-defined chain directions. The boundary of the molecule was determined from a contoured electron density map, and B.C. Wang's automated package[25] for solvent flattening was employed to improve the quality of the MIR map. This procedure increased the average figure of merit from 0.71 to 0.83. The resulting Fourier map showed clear solvent–protein boundaries along with well defined electron density for extended β-strands.

TABLE Ib. Summary of MIR Refinement*

Derivative	Site	x	y	z	Q	P	R_c	FH/residual
$Hg(CN)_4$	1	.2297	.3704	.0956	27.13	53.93	0.550	2.32
	2	.1839	.5042	.2464	23.21	38.25		
$Pt(CN)_4$	1	.2332	.3589	.0772	17.08	51.96	0.461	2.89
	2	.1478	.0431	.0778	18.65	15.99		
	3	.0821	.8733	.0593	22.04	5.78		
Hg-mutant	1	.1434	.4828	.2247	35.36	26.56	0.686	1.59
	2	.3898	.3061	.1174	6.07	7.7		
	3	.4999	.1779	−.006	5.94	16.28		
	4	.4966	.1560	−.032	9.11	14.93		

*x,y,z, fractional cell coordinates; Q, isotropic temperature factor; P, relative occupancy; R_c, centric R factor; FH/resid = $\Sigma\, FH/\Sigma\,|FH$ obs. − FH calc.|. The overall figure of merit is 0.71.

FRODO[26,27] which uses a protein database of best refined protein structures, was used in order to interpret the electron density map. The ridge lines of the map ("bones") were obtained by connecting sets of points through the centroids of the continuous segments of density. FRODO allows the resulting map skeletons to be identified as probable main chain, possible main chain and side chain. Initially the chain was modeled as polyserine and later modified to the appropriate residues. Whenever the connectivity showed a loop or a turn, a database search within FRODO was used to place the fragments in the background, a helpful aid in building the difficult parts of the model.

Molecular Dynamics and Conventional Refinement

This 3.0 Å model was refined initially with X-PLOR,[28] which employs molecular dynamics coupled with energy minimization techniques, operating on an Alliant FX 80 computer. Two different simulated annealing (SA) strategies were adopted. As a first choice the two undefined loops (51–55 and 118–125) were removed and the rest of the molecule was treated as three separate fragments. Simultaneously as a second strategy, these loops were built by using the built-in FRODO database (even though a few residues did not have reliable density), and the whole molecule was subjected to the SA procedure. The initial R-factor before starting the simulated annealing was 47%. Conditions set were (1) the number of steps of energy minimization was 240 with $\Delta F = 0.05$ Å (ΔF indicates how far any atom can move before the first derivative of the energy term due to diffraction data is updated); (2) heating stage of molecular dynamics, 0.5 psec, $T = 4{,}000$ K, timestep = 1 fsec, velocity scaling every 25 fsec, and ΔF of 0.2 Å; (3) cooling stage of molecular dynamics, 0.25 psec, T = 300 K, timestep = 1 fsec, velocity scaling every 25 fsec; and ΔF of 0.2 Å, (4) with 150 steps of energy minimization and $\Delta F = 0.05$ Å. The first stage of SA revealed a weak but continuous density in the above said surface loop regions, for both the strategies, and the R-factor dropped from 47 to 32%. The resulting map enabled the ambiguous loops to be built. For the second stage of SA, data were extended to 2.5 Å. For the last stage the T was kept as 1,000 K. Computed $4F_o - 3F_c$ and $F_o - F_c$ maps confirmed the locations of the ambiguous parts of the molecule, especially the surface loop regions. At the end of the SA refinement the R-factor was 25%.

The model was then subjected to restrained least-squares refinement program RESTRAIN,[29,30] running on the Alliant FX80 computer. Minimum target interatomic restrain distances were used to remove unfavourable van der Waals contacts. Planarity restraints were applied to aromatic rings, side chain carbonyls, and amides, and, to a lesser degree, peptide planes of the main chain. Progress was monitored by a calculation of the crystallographic R-factor

$$R = \frac{\Sigma||F_o| - G|F_c||}{\Sigma|F_o|}$$

where G is a scale factor. Structure factor amplitudes were weighted by the modified Cruickshank function,[31]

$$W_f = \frac{W_{f1} \times \left(\frac{\sin\theta}{\lambda}\right)^{W_{f2}}}{W_{f3} + |F_o| + W_{f4}|F_o|^2}$$

where the W_f values were chosen to give a uniform distribution of $W\Delta F^2$ with respect to resolution and amplitude. The weights of the distance restraints at the end of the refinement were adjusted such that the rms deviations of the target values from the ideal values were as small as possible. Atomic coordinates, an overall scale, and an overall temperature factor were refined for the first few cycles and only later were individual isotropic temperature factors allowed to change. At this stage, unidentified peaks in the difference Fourier maps were assigned to water molecules. A total of 55 such water molecules were identified and included in subsequent refinement. The least-squares refinement was performed progressively by increasing the resolution of the data from 2.5 to 2.0 Å. Throughout the refinement the weights for the geometric restraint classes were varied in order to obtain a model with reasonable geometry and expected rms deviation. Sixty additional water molecules were identified during further cycles of refinement and remodeling to electron density maps.

ANALYSIS OF THE STRUCTURE

The final R-factor for reflections between 20 and 2.0 Å resolution is 0.19. The error in the atomic coordinates is estimated to be 0.23 Å by the method of Luzzati.[33] The deviations observed in the final model for bond lengths, bond angles and for planar groups are found to be well within the ideal targeted variances. Atomic coordinates have been deposited with the Protein Data Bank.[32] Finzel et al.[20] and Priestle et al.[19] also submitted their coordinates simultaneously and a comparison of our structure with these two revealed that the three are almost identical with a few deviations in the surface loops. The root mean square deviations between our structure and the other two are 0.33 and 0.39 Å, respectively.

Figure 1 shows the main chain torsion angles (ϕ,ψ) plotted in the conventional way,[34] with potential energy contours superimposed. With the exception of a few residues, most of the main chain ϕ,ψ angles are in the allowed regions for L-amino acids.

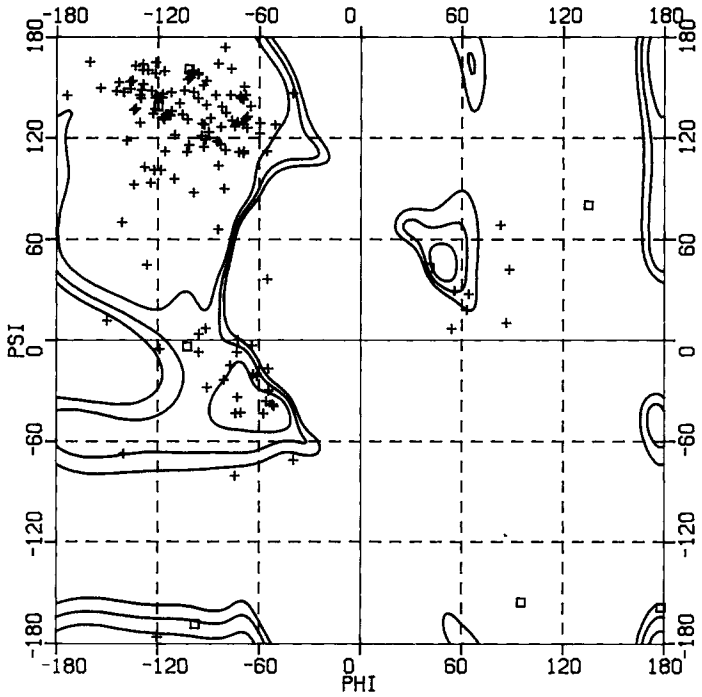

Fig. 1. Ramachandran plot (ϕ,ψ) of the main chain of interleukin-1β, along with the superimposed isoenergy surface contours. The contours are at 4, 6, 8 kcal/mol of the "alanine dipeptide." Glycine (□) and the rest are (+).

One of the 8 proline residues, Pro-91, has a *cis* conformation, with ϕ,ψ angles of −84° and 164° (as observed in the other two structures). The ϕ,ψ angles of the other proline residues cluster around −65°, 143°, with two exceptions: Pro-87 (−73°, 0°) and Pro-2 (diffuse density and high thermal parameters, with unreliable angles). The χ_1 values of the side chains in interleukin-1β adhere to the favored trimodal distribution with peaks at 60° and 180° and a maximum population around 300°.

Isotropic thermal parameters (B) were refined for all nonhydrogen atoms including solvent oxygen atoms. As expected, the main chain atoms have lower mean B values than side chain atoms. The mean B value for all 1,219 protein atoms is 38.1 Å^2 and that of 612 backbone atoms is 33.95 Å^2. The regions of the molecule showing the highest B values are mainly in loops connecting β-strands (residues 33–35, 49–54, 106–108, and 137–141) and residues near the amino and carboxy termini. The same characteristics of high thermal fluctuations in the same segments of this molecule have been observed in the other two reported structures.

Of the well defined 115 solvent molecules identified, nine are internal, bound tightly within the cavities of the protein. Fifty-one solvent molecules are in the first solvation shell, interacting directly with the protein's main chain or side chains. The remaining waters are either in the second shell or between symmetry-related molecules in the crystal lattice. Crystal packing analysis shows that long uninterrupted solvent channels run parallel to the crystallographic a and b axes. The residues of high static accessibility to the solvent[35] are indicated in Figure 2. As expected almost all the charged residues show a much larger accessibility than the mean, while hydrophobic residues, Val, Leu, Ile, and Phe are less accessible than the mean. Glycines and prolines display a high mean accessibility. All the tyrosines are exposed and make hydrogen bonding contacts with solvent molecules.

OVERALL ORGANIZATION OF THE MOLECULE

The molecule resembles a conical barrel with a shallow open face on one end and a closed face on the other. The backbone atoms of the completed model, viewed parallel and perpendicular to the barrel axis, are shown in Figure 3a and b, respectively. The molecule contains 12 antiparallel β-strands, whose overall fold is similar to that of Kunitz-type soybean trypsin inhibitor.[36,37] This kind of folding pattern has been classified as the "IL-1 fold."[22] The secondary structural elements assigned based on the definitions of Kabsh and Sanders,[38] are shown in Figure 4. The overall structure of the molecule consists of three similar fragments (F1, F2, F3), each containing two pairs of β-strands. Three pairs of β-strands (one pair from each of the fragments) form the six-stranded barrel; the other three pairs cover one end

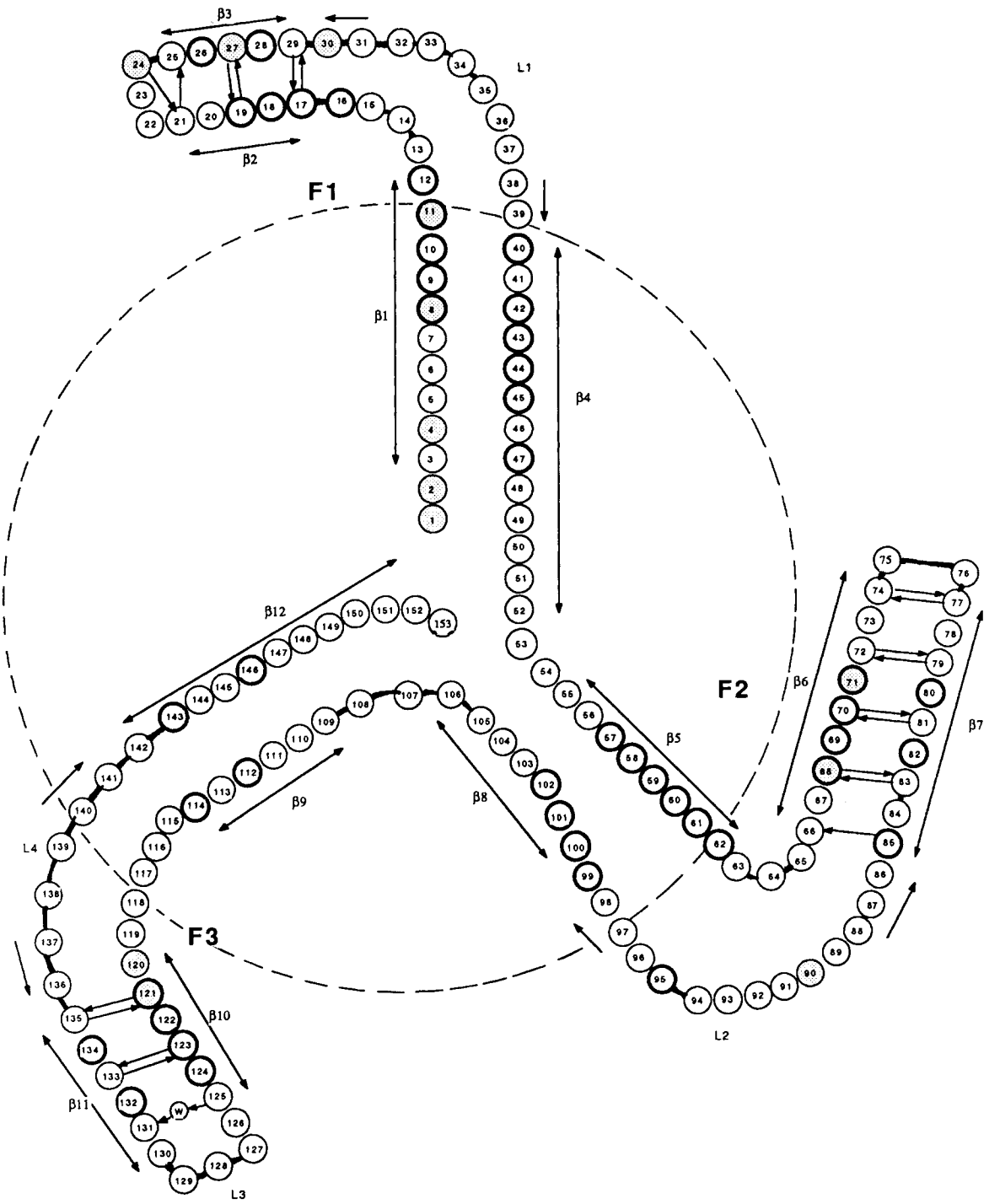

Fig. 2. A schematic drawing of the interleukin-1β molecule showing the three fragments (F1, F2, F3) that are related by a pseudo-3-fold symmetry. All the strands from β1 to β12 are also marked. The strands within the dotted circle (β1, β4, β5, β8, β9, β12) are the staves of the barrel. The strands outside the circle (β2, β3, β6, β7, β10, β11) form the flaps closing the barrel at the "closed end." The highlighted residues are not accessible to the solvent; the others are exposed. The reported mutants are highlighted within the circle. The hydrogen bonds shown are responsible for the formation of the β-hairpins. Refer to Finzel et al.[20] for the detailed hydrogen bonding scheme. The numbering of the strands and the residues that constitute them are β1 = 3–12, β2 = 17–21, β3 = 25–29, β4 = 40–52, β5 = 55–62, β6 = 66–74, β7 = 77–85, β8 = 100–106, β9 = 109–114, β10 = 120–125, β11 = 130–135, and β12 = 142–152. Similarly the β-turns are T1 = 12–15, T2 = 21–24, T3 = 33–36, T4 = 34–37, T5 = 35–38, T6 = 52–55, T7 = 62–65, T8 = 74–77, T9 = 86–89, T10 = 106–109, T11 = 114–117, and T12 = 117–120. There are four loops represented as L1 = 30–39, L2 = 86–98, L3 = 125–131, and L4 = 136–141.

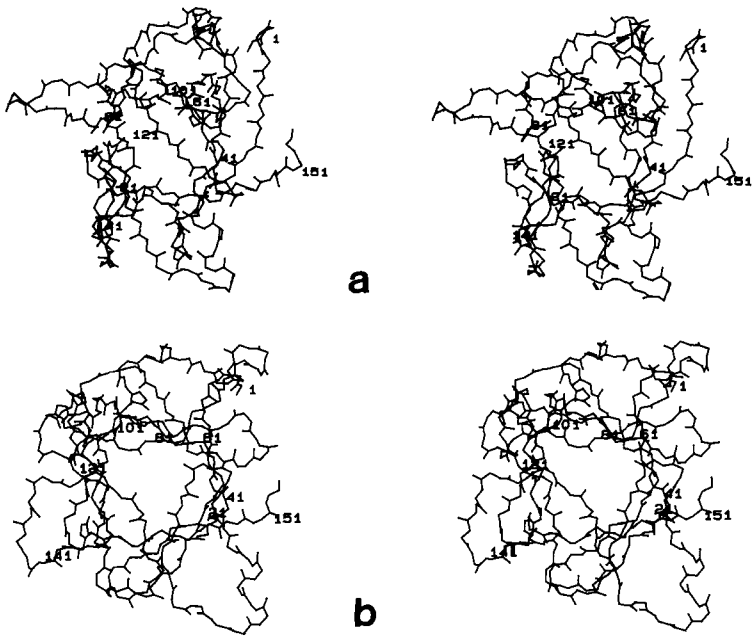

Fig. 3. Stereo-plot of the main chain atoms of IL-1β, **(a)** viewed parallel to the axis of the barrel and **(b)** viewed perpendicular to the axis.

of the barrel, henceforth referred to as the "closed end." The amino and carboxy termini are close to each other at the "open end" of the barrel. The length of the long tubular core of the molecule is about 23 Å. A space filling model of all the atoms at the open end is shown in Figure 5. For the sake of consistency, the nomenclature for the secondary structural elements of this molecule is taken from Finzel et al.[20] The molecule has internal pseudo-3-fold symmetry, with each subunit (F1, F2, F3) having a ββββLβ motif (Fig. 2). Residues 1 to 52 (F1), 53 to 107 (F2), and 108 to 153 (F3) form these fragments. These ββββLβ motifs can be superposed with structural similarities (Fig. 6). Pairwise superposition of topologically equivalent residues of these three fragments and their mean deviations are listed in Table II. The residues responsible for the formation of the sheets are well conserved, whereas the connecting loops show large variability.

The molecule is made of 12 β-strands, where six of these (β1, β4, β5, β8, β9, and β12) constitute the antiparallel β-barrel. Richardson[39] classified the fold of the soybean trypsin inhibitor, which is very similar to this molecule, as pure up-and-down β-barrel with a simple $+1_6$ topology. There are five β-hairpins in this molecule, two of them in the open end and three at the closed end. Residues 18 to 28, 69 to 82, and 122 to 135 form the three β-hairpins at the closed end wherein three strands (residues 24–28, 78–82, and 129–135) are in close proximity as three sides of a triangle, covering this end of the barrel (Fig. 4). Twenty-four hydrophobic side chains line the inner surface of the barrel, including eight leucines, one isoleucine, one valine, and six phenylalanines. Most of the aromatic groups have their planes aligned along the barrel axis and both the ends of the barrel have concentrations of exposed polar residues.

STRUCTURE–FUNCTION RELATIONSHIP: A HYPOTHESIS

The accepted function of interleukin-1 is as a mediator of intercellular communication within the immune and related systems. To better understand these processes we seek to identify the functional parts of this molecule and to explain the binding interactions with IL-1's specific receptor. The IL-1 receptor has been identified; its extracellular portion contains three immunoglobulin-like domains with which IL-1 binds in order to induce the "IL-1-related physiological responses."[40] The following observations, derived from the literature, lead us to conclude that the IL-1 binding site is large, similar to the binding region in antigen–antibody complexes where epitopes of approximately 700 Å^2 in surface area,[41,42] formed by various segments of the immunoglobulins, participate in the binding of antigens. First, even though there exists two types of IL-1 (IL-1β and IL-1α), with similar structures, both bind to the same cell surface receptor and exert similar activities. Second, site-directed mutations of residues well separated from one another reduce the binding. Third, peptide analogs of different lengths based on IL-1's primary sequence (from residues 47–55, 121–153) showed only limited activity in T-cell activation assays.[43,44] Analysis of the surface of IL-1

reveals an epitope consisting of many polar residues widely spaced, approximately in an annular fashion, around the open end of the barrel. The core of the barrel, though doubtfully involved in binding, must nevertheless be important to the function of IL-1, since mutations within it reduce activity but not binding. Although it is not known how binding leads to cell activation, a central tenet of our hypothesis is that binding and function (cell proliferation through signal transduction) involve separate regions of the IL-1 molecule: the surface polar loops are required for the binding and the core of the barrel is required for the physiological response. The structural evidence in support of this hypothesis is discussed below.

Proposed Binding Surface

The open end of the barrel, which is proposed to be the receptor-binding surface, has a broad surface area (Figs. 5, 7a, and 7b) containing many polar residues. Residues from six β-turns [type 1 β-turn 1 (T1 = 11–17), type III β-turn 3 (T3 = 33–36), type I β-turn 6 (T6 = 52–55), type I β-turn 7 (T7 = 62–65), type I β-turn 9 (T9 = 86–89), type I′ β-turn 10 (T10 = 106–109)] are present in this open end (Fig. 7a and b). There is a β-bulge between strands β4 and β5 in one of the hairpins; this bulge may play a key role in the formation of the putative binding surface. Richardson[39] describes a β-bulge as a "region between two consecutive β-type hydrogen bonds that includes two residues on one strand opposite a single residue on the other." The β-bulge in IL-1 is of the "wide" type, where the hydrogen bond pairing is interrupted between Val-47 and Ser-52 on one strand and between Pro-57 and Lys-55 on the other. The deviation from the normal pairing is achieved by a water-mediated hydrogen bond between two carbonyl oxygens as 47 Val O . . . W208 . . . O Pro-57. After interruption the pairing continues with the hydrogen bond between 52 Ser N . . . O Lys-55. A "wide" β-bulge could be formed by the shift produced by two or three residues, whereas in this bulge region there is a six residue shift. This kind of large deviation in the pairing is made possible not only by the presence of the prolyl ring between the strands but also by a hydrogen bond and a salt bridge on either end of the strand 48 to 55, as Gln-48 OE1 . . . 3.1 Å . . . NZ Lys-94 and Lys-55 NZ . . . 3.3 Å . . . OE1 Glu-113. In addition to these, there is another hydrogen bond between carbonyl oxygen of 53 and the carboxyl oxygen of 105 as Glu-105 OE1 . . . 3.2 Å . . . O Asn-53. These multiple interactions might be the cause for this "wider" β-bulge, whose conformation is such as to place the side chains of polar residues (Glu-51, Asn-53, Asp-54) in the proposed binding surface, fanning out in the direction of the open end of the barrel. After analyzing similar β-bulges, Richardson[39] points out that "these bulges are often found at active sites, probably because they have a strictly local but specific and controlled effect on side chain direction." The bulge present in IL-1 is unusually large, as explained above, and positions the charged side chains in the open end of the molecule, on the proposed binding surface.

There are two prolines, Pro-87 and Pro-91, in the loop region between residues 86 and 94, having unusual internal coordinates. The ϕ, ψ of Pro-87 are $-73°$, 0°, and a *cis* peptide joins Tyr-90 and Pro-91. Such strains might have been caused by the salt bridges in this loop. The first, between Lys- 92 and Glu-96 (92 Nz . . . 2.7 Å . . . OE1 96), stabilizes the conformation of the turn containing residues Tyr-90–Pro-91–Lys-92 (YPK). This YPK turn is further stabilized by another hydrogen bond between the OH Tyr-90 and the other carboxyl oxygen of 96 Glu (90 OH . . . 2.8 Å . . . OE2 96). Another salt bridge exists between Glu-83 and Arg-98 (83 OE2 . . . 3.0 Å . . . NH1 98). Also the amide carbonyl of Gln-48 (from strand β4) forms a hydrogen bond with the amino group of Lys-94 (48 OE1 . . . 3.0 Å . . . NZ 94). Apart from these interactions, carbonyl oxygen of 85 on one other side of the loop makes a hydrogen bond with the side chain amino group of Asn-66 (66 ND2 . . . 2.9 Å . . . O 85). All these interactions serve to stabilize the strained conformation of this loop (between 86 and 94), presenting the side chains of Asp-86, Lys-88, Asn-89, and Lys-93 at the open end of the barrel. Strains in a molecule (residues having abnormal ϕ,ψ values, with defined electron density) often may be related to functional properties and are observed either in the active site or in the region responsible for its activity.[45] The reason for having such strains in this loop may be to place these charged side chains in the putative receptor binding surface.

A similar situation also exists in another region between β8 and β9 (residues 102 and 113), where Asp-145 and Phe-146 deviate from their peptide planarity by about 30°, predisposing the aspartyl side chain of 145 for an electrostatic interaction with the Nz of Lys-109. Two other salt bridges also exist in this region as Glu-111 OE1 . . . 3.1 Å . . . NZ Lys-138 and Glu-113 OE1 . . . 3.3 Å . . . Nz Lys-55. In fact both carboxyl oxygens of Glu-113 interact with Lys-

Fig. 4. The secondary structural elements of IL-1β, as defined by Kabsh and Sander,[38] with the view down the axis of the barrel. The "closed end" is at the farther end of the barrel. The picture was produced by the program "RASTER 3D" written by D. Bacon.

Fig. 5. A space filling model of the "open end" of the molecule, being proposed as the receptor binding surface. Color scheme: white, main chain atoms; red, negatively charged residues; blue, positively charged residues; green, brown, gray, hydrophobic residues; orange, pink, polar residues. The center of the open end of the barrel could be seen as a cluster of charged residues (dark colored) surrounded by white colored main chain atoms. The picture was produced by the program "RASTER 3D" written by D. Bacon.

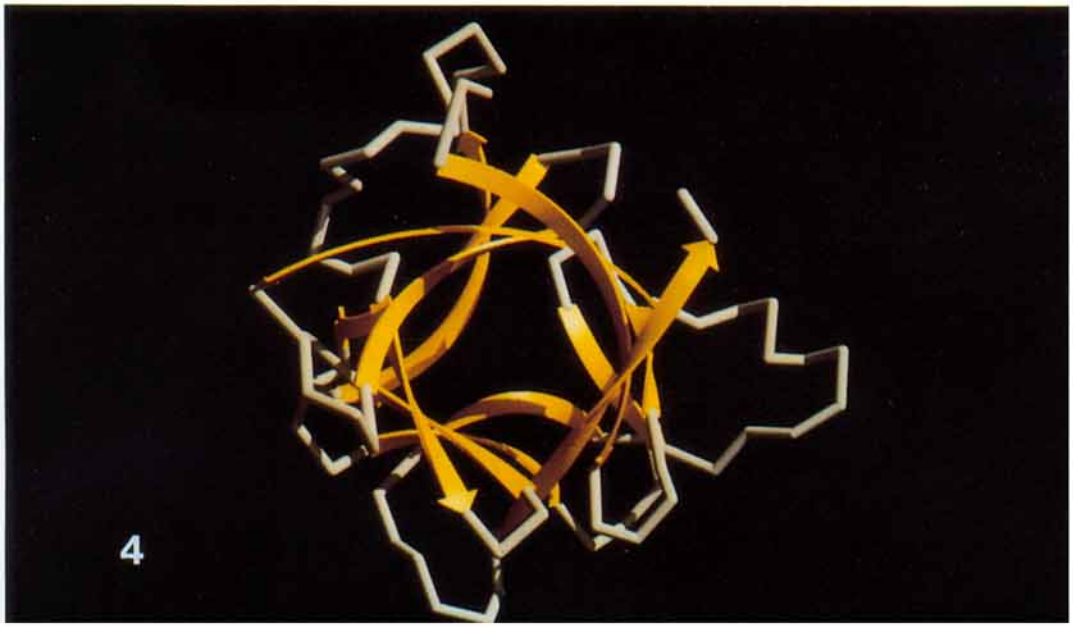

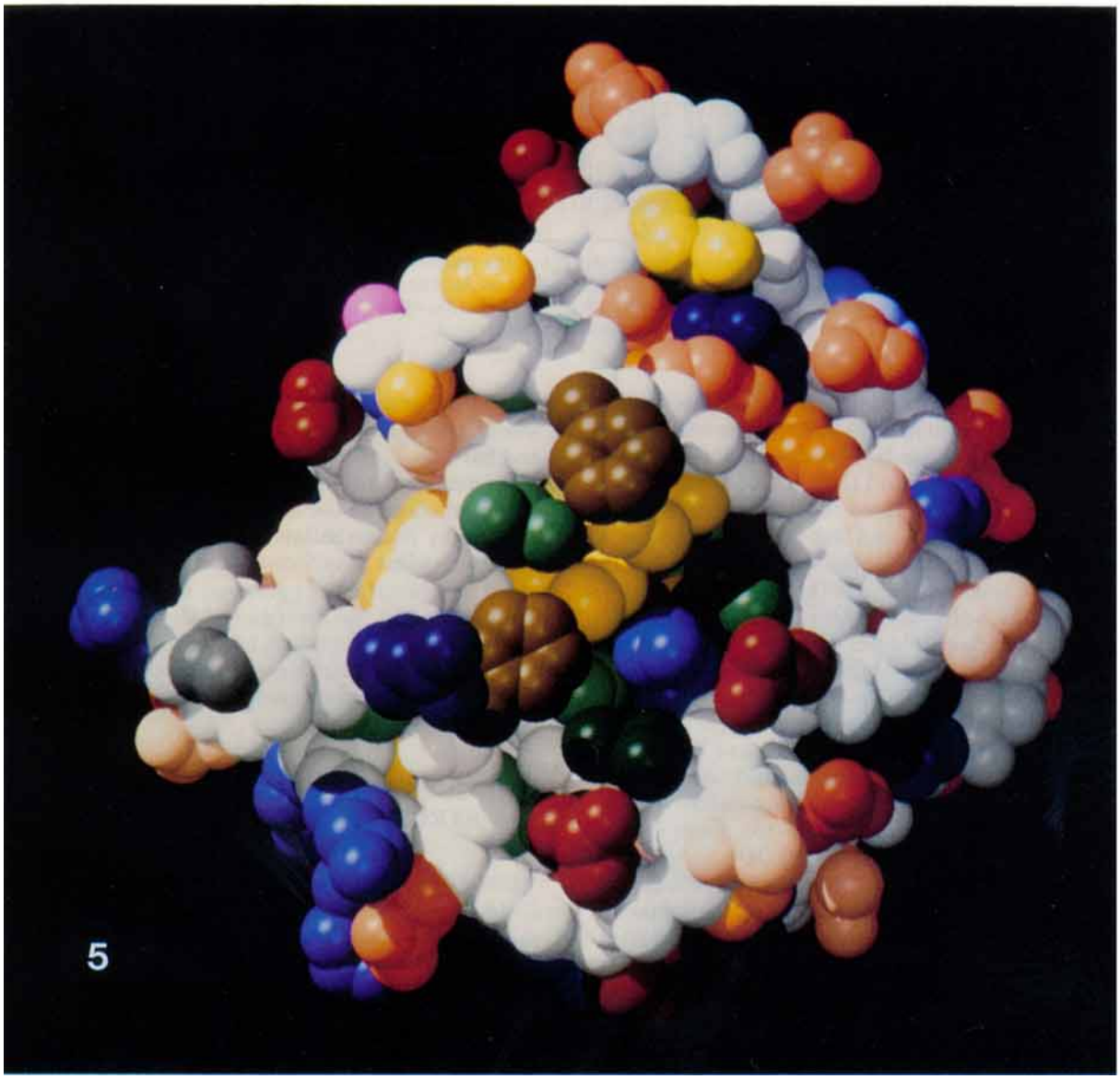

Figs. 4 and 5. Legends appear on page 16.

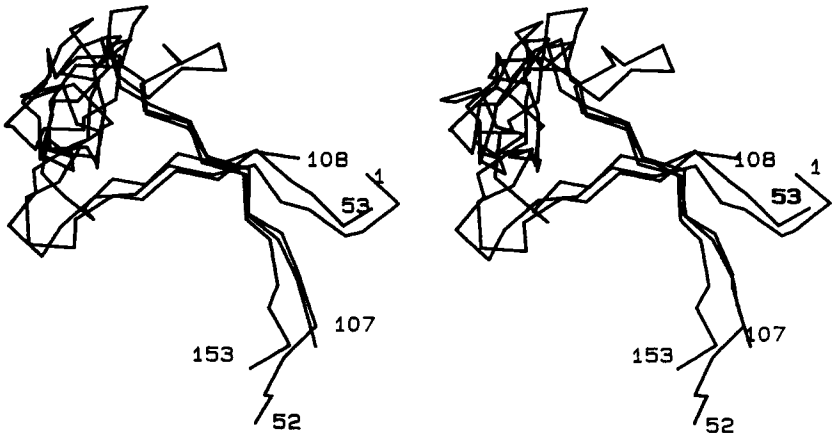

Fig. 6. Stereo-plot of the α-carbon atoms of the three superposed fragments, residues 1–53 (F1), 54–107 (F2), 108–153 (F3).

TABLE II. The Aligned Sequences of Topologically Equivalent Structural Units of the Three Fragments (F1, F2, F3) of IL-1β*

F1	B1	L6	N7	C8	T9	L10	R11	D12	B2	K16	S17	L18	V19	M20	S21	G22		
F2	B5	I56	P57	V58	A59	L60	G61	L62	B6	L67	Y68	L69	S70	C71	V72	L73		
F3	B9	N108	K109	L110	E111	F112	E113	S114	B10	W120	Y121	I122	S123	T124	S125	A127		
Md (in Å)		2.5	1.5	1.0	1.3	1.6	2.5	3.0		1.8	1.4	1.4	2.0	2.3	2.7	2.4		
F1	B3	E25	L26	K27	A28	L29	H30	L31	B4	Q39	V40	V41	F42	S43	M44	S45	F46	V47
F2	B7	T79	L80	Q81	L82	E83	S84	V85	B8	R98	F99	V100	F101	N102	K103	I104	E105	I106
F3	B11	P131	V132	F133	L134	G135	G136	T137	B12	I143	T144	D145	F146	T147	M148	Q149	F150	V151
Md (in Å)		3.5	2.5	2.0	1.6	2.0	2.6	2.3		2.7	1.3	1.0	0.5	0.4	1.2	2.2	2.6	3.2

*The alignment was done by least-squares superposition of the C_αs of the fragments. The first block contains residues from the equivalent srands β1, β5, β9, and the fourth block contains residues from strands β4, β8, β12; all these six strands form the central β-barrel structure and the rest of the six strands (β2, β6, β10, β3, β7, β11) form the other three sheets covering the "closed end." The mean deviation (Md) of either of the C_αs from the central one is also listed.

55 from strand β5, Asn-102 from β8, and the amide nitrogen of 119 from β10, by making one salt bridge and two hydrogen bonds. These favorable interactions stabilize the 102 to 113 loop, and their conformation is such as to orient the side chains of Lys-103, Glu-105, Asn-107, and Asn-108 in the proposed surface at the open end of the barrel.

There is a short 3_{10}-helix in the region between β3 and β4 (residue Gly-33 and Gln-39). Apart from the main chain hydrogen bonds responsible for this helix, there exist two other hydrogen bonds, Asp-35 OD1 . . . 2.7Å . . . NE2 Gln-38 and Arg-11 NH1 . . . 2.9 Å . . . OE1 Gln-39. By such a conformation, residues Gln-32, Gln-34, and Glu-37 have their side chains in the proposed binding surface. Apart from the main chain hydrogen bonds responsible for the formation of the β-hairpin T1 (11–15), a salt bridge made by the Asp-12 and Lys-16 (12 OD1 . . . 2.7 Å . . . Nz 16) adds to its stability. This arrangement places the side chains Arg-11 and Gln-15 in the proposed epitope. In addition, the β-turn between 62 and 65 is folded in such a way that the charged groups of the residues Lys-63, Glu-64, and Lys-65 present themselves on the proposed binding surface. Furthermore, the amino and carboxy termini also form a part of the proposed epitope, contributing the polar side chains of Arg-4, Ser-5, Asn-7, Gln-149, Ser-152, and Ser-153.

In summary, the electrostatic and hydrogen bonding interactions in the loops between strands, made possible by unconventional strains, allow the polypeptide to adopt a conformation that enables an unusual concentration of polar and charged groups to be presented at the open end of the barrel. Such a cluster of charged residues around an area which is almost perpendicular to the barrel axis (Fig. 7a and b) forms a hydrophilic patch with which IL-1 might bind to the receptor.

IN SUPPORT OF THE PROPOSAL (OR) STRUCTURAL IMPLICATIONS OF THE MUTANTS

Site-directed mutagenesis has been carried out on IL-1β in order to identify residues that play important roles in its activity.[46–52] Mutants of the following residues were prepared: Ala-1 (117), Pro-2 (118), Arg-4 (120), Cys-8 (124), Arg-11 (127), Tyr-24 (140), Lys-27 (143), His-30 (146), Tyr-68(184), Cys-71 (187), Tyr-90 (206), Trp-120 (236), Tyr-121 (237),

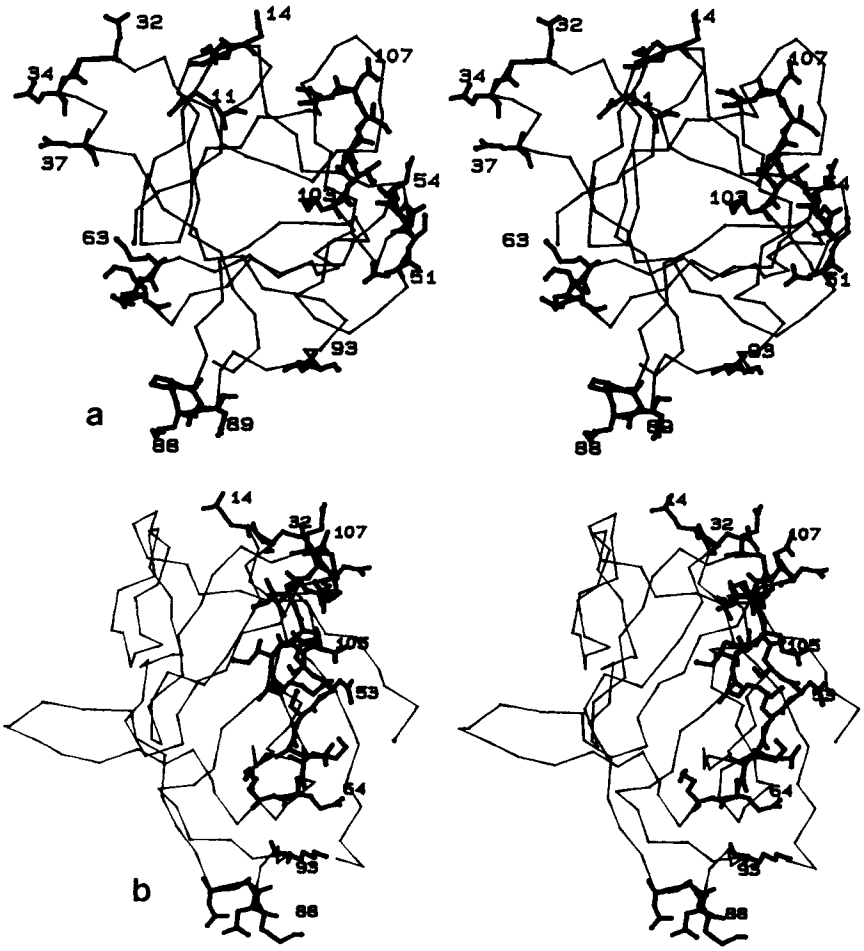

Fig. 7. Stereo-diagram of all the α-carbon atoms of the molecule along with the polar/charged side chains that form part of the proposed receptor binding surface. **(a)** Viewed down the axis of the barrel and **(b)** perpendicular to the axis.

and Lys-138 (254) (the number within the parentheses is that of the prosequence). The results of the mutations can be classified as (1) mutations leading to decrease in IL1 activity [R4E, C8X, C71X, R11G, K138C] or increase in activity [A1T,P2M] (Fig. 8a) and (2) mutations leading to a reduction in IL-1 binding [R4E, R11G, H30Q, H30N, H30R] or increase in binding [P2M] to the receptor without altering activity (Fig. 8b) (letter X indicates that the residue has been deleted). Table III lists the mutations and their effects on binding and activity.

Of the mutants that led to the decrease in activity, Arg-4 and Cys-8 are in the amino terminal β1 strand; their side chains are placed almost at the center of the open end of the barrel. The Arg-4-Glu mutant has only 0.15% activity relative to that of the wild-type protein. By changing a positively charged side chain of Arg-4 to a negatively charged side chain of Glu results in a change in the electrostatics of the proposed binding surface, implying that the charges aligned along the axis of the barrel play a crucial part in IL-1 activity.

Cysteine Mutants

There are two free cysteines in this molecule, one of which, Cys-8, is at the open end of the barrel. The Cys-8-Ala mutant did not appear to result in any significant change in the activity, whereas deleting Cys-8 or changing Cys-8 to Ser reduced the activity by 33-fold.[50] The sulfur atom of the side chain of Cys-8 is surrounded by two other sulfur atoms from the side chains of Met-44 and Met-148. Conversion of Cys to Ala has no effect on the structure other than at the site of mutation as evidenced from the electron density map obtained at 2.0 Å resolution.[53] However, it is reasonable to expect that deleting the side chain of Cys-8 would distort the arrangements of its neighboring side chains within the barrel. That such a rearrangement directly influences the

TABLE III. Summary and Location of the Mutations Carried out on IL-1β Molecule*

Mutants	Binding (%)	Activity (%)	Location	Reference
IL-1β (wild)	100	100		
C8 → S	—	2.7	β1	50
C8 → A	—	100	β1	50
C8 → deleted	—	3.2	β1	50
C8/C71 → A/S	—	110		50
C8/C71 → A/A	—	100		50
C71 → S	—	95	β6	50
C71 → A	—	105		50
C71 → deleted	—	0.1		50
R11 → G	75	1.0	β1	52
K27 → C	100	100	β3	51
K138 → C	100	33	β11–β12	51
A1T	—	380	β1	48,49
A1/P2 → T/M	200	700	β1	48,49
A1/P2/R4 → T/M/E	0.20	0.14	β1	48,49
Y24 → F	100	—	β2–β3	46
Y68 → F	100	—	β6	46
Y90 → F	100	—	β7–β8	46
W120/Y121 → F/F	100	—	β10	46
H30 → Q	50	—	β3	46
H30 → N	3	—		46
H30 → R	1	—		46

*The activity and binding are represented as percentage relative to the wild type IL-1β.

IL-1 activity suggests that the residues along the barrel axis are important for its function. Why the Cys-8-Ser mutant has reduced activity is more difficult to understand. The problem unlikely is steric since Ser is nearly isoteric with Cys and our crystallographic results from this mutant did not reveal any significant structural change. It may be that the replacement of the sulphur atom by an oxygen leads to an electrostatic perturbation at the barrel end which in turn causes a change in the activity but not in binding.

Cys-71 is partially exposed to a first-layer water molecule W269 and also at a distance of 3.6 Å from an internal water molecule W210. The side chain atom SG of Cys-71 is surrounded by the side chain of Ser-114, the carbonyl oxygen of 98, and the side chains of Leu-80, Leu-134, and Phe-101. Mutation of this cysteine to Ala or to Ser did not cause any profound change in the activity but when deleted inactivates IL-1 completely.[50] Deleting this residue likely changes the outer cover of the barrel, thereby exposing its inner core to the external solvent. This suggests that the external envelope to maintain the inner hydrophobicity of the barrel is important for its function.

Arg-11-Gly

The Arg-11-Gly mutant showed a 100-fold reduction in bioactivity whereas its receptor binding activity was decreased only by 25%.[52] The side chain of Arg-11 is on the proposed binding surface making an interaction with Gln-39 as 11 NH1 . . . 2.9 Å . . . OE1 39. Further this network is extended as Gln-39 NE2 . . . 2.7 Å . . . W209 . . . 2.7 Å . . . W207. These two internal water molecules, W207 and W209, are nearer to the barrel axis. Changing Arg-11 to Gly possibly disrupts the above network of hydrogen bonds, exposing the inner barrel via these internal waters, in turn lowering the activity. It is also conceivable that such a mutation can cause a rearrangement of the loops (13–16, 31–39), due to the loss of the above salt bridge, thereby altering the positions of side chains, which are also part of the proposed receptor binding epitope. Such rearrangements in turn would directly affect the receptor binding. The reason for only partial reduction in binding is probably because conversion of Arg-11 to Gly results in the elimination of only one of many polar interactions involved in receptor binding.

Lys-138-Cys

Mutation of Lys-138 to Cys reduces the activity 3-fold but does not affect the receptor binding.[51] Lys-138 is situated away from the open end of the barrel, held tightly by a salt bridge with Glu-111 (Lys-138 NZ . . . 3.1 Å . . . OE1 Glu-111). Between the side chain of 138 and the barrel axis there is an internal water W215. Converting Lys to Cys breaks the above said salt bridge and likely exposes the inner barrel to the external solvent. This expected solvation of the barrel core, along with the experimental evidence of reduction in activity, supports the idea that the exclusion of external solvent from the inner barrel is vital for IL-1's function. That the mutation has no influence in the binding suggests that Lys-138 is not part of the receptor-binding region.

Lys-27-Cys

Changing Lys-27 to Cys-27[51] results in no change in activity or in binding. Lys-27 is at the closed end of the barrel with its side chain extending into the solvent region. Even though the polar side chains of Ser-21, Glu-25, and Asn-129 are present in the vicinity of the Lys-27 side-chain amino group, none of the neighboring residues is within hydrogen bonding distance. That IL-1's activity has not been influenced by this mutation suggests that this residue is not directly taking part in the functional part of the molecule. In fact, such a conversion would not disrupt the barrel core. Modification caused no change in binding to support the idea that the receptor-binding surface is not near this residue.

N- Terminal Mutations

Mutations of residues in the amino terminal region affect the activity.[48,49] The double mutant Ala-1-Thr and Pro-2-Met (A1T/P2M) increases the activity. In the crystal structure these residues have a diffuse density with high thermal parameters, suggesting that they are quite mobile. It seems that any

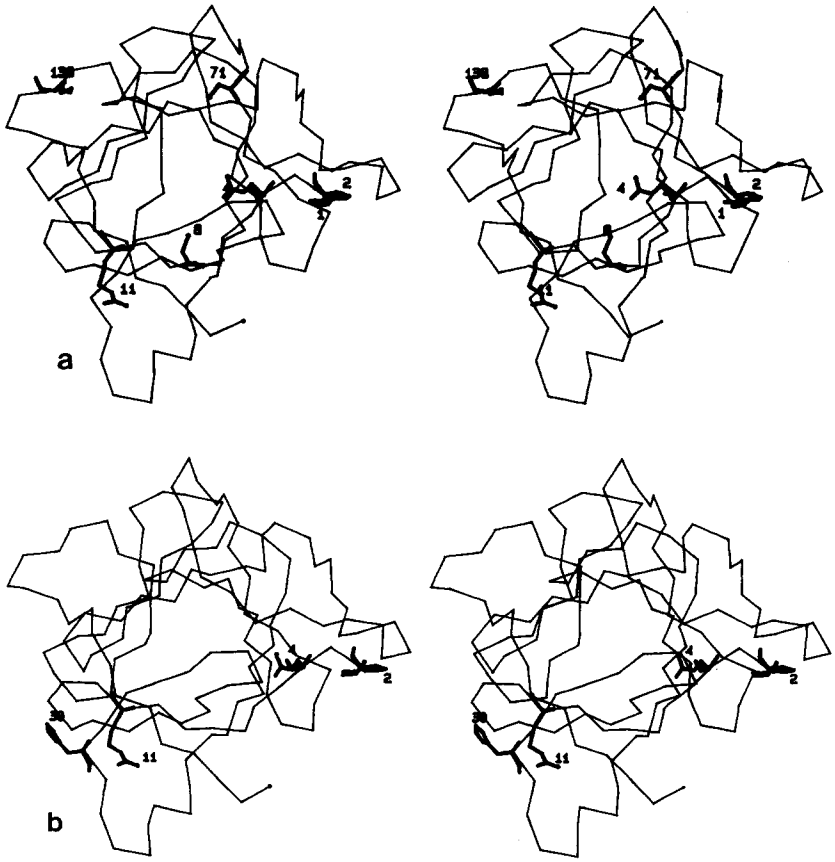

Fig. 8. Stereo-diagram of all the α-carbon atoms of the molecule along with the reported mutants of the side chains of the native molecules. **(a)** The mutations resulting in reduction in activity [Arg-4, Cys-8, Cys-71, Arg-11, Lys-138] or increase in activity [Ala-1, Pro-2]; **(b)** the side chains of the residues which when mutated decreased the binding [Arg-4, Arg-11, His-30] and increased the binding [Pro-2].

alterations of charges at the open end of the barrel will lead to a change in the electrostatic field around the molecular axis, in turn causes a change in the activity. Mutating the N-terminal sequence from Ala-1–Pro-2–Val-3–Arg-4– to Thr-1–Met-2–Val-3–Glu-4– led to a reduction of the activity by 600-fold (Table III), further supporting the idea that an appropriate electrostatic environment near the open end of the barrel is a requirement for its activity.

Aromatic Mutations

Mutation of the tyrosines to phenylalanines (Y24F, Y68F, Y90F, W120/Y121, to F/F) did not cause significant loss of activity.[47] All of these residues are located at the closed end of the barrel, opposite to the proposed receptor-binding site. The results of this set of mutations indicate that the closed end of the barrel is not directly involved with activity or in binding. Even if the aromatic residues underwent some small rearrangements, as evidenced by NMR spectroscopy,[47] these would not affect the barrel core or the proposed receptor binding surface.

His-30 Mutations

Conversion of His-30 to Gln, Asn, or Arg (H30Q, H30N, H30R) showed a reduction in the binding of IL-1β to its receptor[46] but did not influence the activity. His-30 is neither in the proposed receptor binding surface nor inside the barrel but is on the outer surface of the barrel, bridging two of the loops with residues 11–17 (T1) and 125–131 (L3). ND1 of His-30 forms a hydrogen bond with the carboxylate of Glu-128 (128 OE2 . . . 2.6 Å . . . ND1 30), while NE2 is hydrogen bonded to the carbonyl of Gln-14(30 NE2 . . . 3.0 Å . . . O 14). The loop between residue 30 and 39 (L1) is completely exposed to the solvent and His-30 with its twin interactions on one side and Gln-39's electrostatic interaction with Arg-11 on the other side stabilizes this loop within the molecule as L3–L1–T1. Mutating His-30 causes disruption of these stabilizing interactions and likely alters the conformation of the L1 loop. Such rearrangement in turn displaces residues Gln-32, Gln-34, Glu-37, Met-36 of L1 and Asn-15 of T1: the residues in the proposed receptor-binding surface causing a reduction in the binding. His-30 mutation

has not affected the IL-1 activity, suggesting that its location, away from the core of the barrel, is not in the molecule's functional part.

Peptide Analogs

Many peptide fragments have been made, either by chemical synthesis or by the use of recombinant DNA techniques, and have been tested for biological activity.[43,44,54–60] Even though these fragments showed a limited activity in T-cell activation assays, they could not duplicate the native protein's response. We suggest that the reason why these peptides did not mimic IL-1 activity is that the entire β-barrel structure is required for both binding and activity. In this respect it could be possible that IL-1–receptor interactions resemble that of antibody–protein antigen interactions, where contact involves a large surface area. This is in sharp contrast to the peptide hormone–receptor or neurotoxin–receptor interactions where a relatively short peptide segment is responsible for binding and activity.

CONCLUSION

After analyzing the three-dimensional structure and the available literature on IL-1 we believe that a large epitope containing many polar and charged groups at the "open end" of the barrel forms the receptor binding surface. The core of the barrel seems to be the functional part, by which IL-1 transmits its signal for cell proliferation. A better understanding of how the immune response is stimulated by IL-1 upon its binding to its receptor molecule is imperative in designing drugs for many diseases. We hope that the obtained molecular structure and our identification of the IL-1–receptor epitope might provide valuable information toward such an aim.

ACKNOWLEDGMENTS

We wish to thank Evon L. Winborne for having grown the crystals of IL-1β. Also we wish to thank Drs. W.J. Stevens and D.T. Gallagher for many helpful discussions and critically evaluating this manuscript. Certain commercial equipment, instruments, and materials are identified in this paper in order to specify the experimental procedure. Such identification does not imply recommendation or endorsement by the National Institute of Standards and Technology, nor does it imply that the materials or equipments identified are necessarily the best available for this purpose.

REFERENCES

1. Dinarello, C.A. Interleukin-1 is produced in response to infection and injury. Rev. Infect. Dis. 6:51–95, 1984.
2. Oppenheim, J.J., Kovacs, E.J., Matsushima, K., Durum, S.K. A review explaining the role of interleukin-1 during immunological and inflammatory processes. Immunol. Today 7:45–56, 1986.
3. Durum, K.S., Oppenheim, J.J., Neta, R. In: "Immunophysiology, Chapter 11, Immunophysiologic Role of Interleukin-1." Oppenheim, J.J., Shevach, E.M., eds. New York: Oxford University Press, 1990:210–225.
4. Dinarello, C.A. Review on the biology of interleukin-1. Adv. Immunol. 44:153–205, 1989.
5. Miller, L., Dinarello, C.A. IL1 plays an active role in promoting inflammation in joints. Pathol. Immunopathol. Res. 6:22–36, 1987.
6. Auron, P.E., Webb, A.C., Rosenwasser, L.J., Mucci, S.F., Rich, A., Wolff, S.M., Dinarello, C.A. Nucleotide sequence of human monocyte interleukin-1 precursor cDNA. Proc. Natl. Acad. Sci. U.S.A. 81:7907–7911, 1984.
7. March, C.J., Mosley, B., Larsen, A., Cerretti, D.P., Braedt, G., Price, P.J., Hopp, T.P., Cosman, D. Isolation of cDNA clones encoding for IL1-α and β. Nature (London) 315:641–647, 1985.
8. Cameron, P., Lumjuco, G., Rodkey, J., Bennet, C., Schmidt, J.A. Aminoterminal processing at Ala 117 of the precursor-interleukin to produce a mature interleukin-1 β. J. Exp. Med., 162:790–801, 1985.
9. Hazuda, D.J., Lee, J.C., Young, P.R. IL1b may be secreted from monocytes as inactive 31Kda precursor and processed later. J. Biol. Chem. 263:8473–8479, 1988.
10. Hazuda, D.J., Strickler, J., Kueppers, F., Simon, P.L., Young, P.R. IL1b precursor can be processed after secretion by several proteases released at inflammatory sites. J. Biol. Chem. 265:6318–6322, 1990.
11. Sleath, P.R., Hendrickson, R.C., Kronheim, S.R., March, C.J., Black, R.A. Human pro-IL1-β is cleaved solely between the residues Asp116-Ala117 (prosequence numbering). J. Biol. Chem. 265:14526–14528, 1990.
12. Mosley, B., Urdal, D.L., Prickett, K.S., Larsen, A., Cosman, D., Conlon, P.J., Gillis, S., Dower, S.K. IL1-*beta* is active only after processing the precursor. J. Biol. Chem. 262:2941–2944, 1987.
13. Dower, S.K., Kronheim, S.R., Hopp, T.P., Cantrell, M., Deeley, M., Gillis, S., Henney, C.S., Urdal, D.L. IL1-α and Il1-β bind to the same receptor protein with similar affinities on target cells. Nature (London) 324:266–268, 1986.
14. Dower, S.K., Call, S.M., Gillis, S., Urdal, D.L. IL1-α and IL1-β bind to the same receptor protein with similar affinities on target cells. Proc. Natl. Acad. Sci. U.S.A. 83:1060–1064, 1986.
15. Kilian, P.L., Kaffka, K.L., Stern, A.S., Woehle, D., Benjamin, W.R., DeChiara, T.M., Gubler, U., Farrar, J.J., Mizel, S.B., Lomedico, P.T. IL1-α and IL1-β bind to the same receptor protein with similar affinities on target cells. J. Immunol. 136:4509–4514, 1986.
16. Matsushima, K., Akahoshi, T., Yamada, Y., Furutani, Y., Oppenheim, J.J. IL1-α and IL1-β bind to the same receptor protein with similar affinities on target cells. J. Immunol. 136:4496–4502, 1986.
17. Giovine, F.S., Duff, G.W. Overview of the biology of IL-1. Immunol. Today 13–20, 1990.
18. Gilliland, G.L., Winborne, E.L., Masui, Y., Hirai, Y. Crystallisation report of IL1-β. J. Biol. Chem. 262:12323–12324, 1987.
19. Priestle, J.P., Schar, H.-P., Grutter, M.G. Refinement on the structure of IL1-β, at 2.0 Å resolution. Proc. Natl. Acad. Sci. U.S.A. 86:9667–9671, 1989.
20. Finzel, B.C., Clancy, L.L., Holland, D.R., Muchmore, S.W., Watenpaugh, K.D., Einspahr, H.M. Crystal structure solution of IL1-β at 2.0 Å resolution. J. Mol. Biol. 209:779–791, 1989.
21. Clore, G.M., Wingfield, P.T., Gronenborn, M. Structure of Il1-β, derived from 3-D NMR spectroscopy. Biochemistry 30:2315–2323, 1991.
22. Graves, B.J., Hatada, M.H., Hendrickson, W.A., Miller, J.K., Madison, V.S., Satow, Y. Structure of interleukin-1 α at 2.7 Å resolution. Biochemistry 29:2679–2684, 1990.
23. Howard, A.J., Gilliland, G.L., Finzel, B.C., Poulos, T.L., Ohlendorf, D.H., Salemme, F.R. Use of an imaging proportional counter is macromolecular crystallography: Algorithm description of XENGEN, a data processing package. J. Appl. Crystallogr. 20:383–387, 1987.
24. Steigemann, W. PROTEIN: Aprogram system for the crystal structure analysis of proteins (Version 85). Ph.D. Thesis, Technical University, Munich, 1974.
25. Wang, B.C. Density modification to improve the phases by solvent leveling. Methods Enzymol. 115:90–112, 1985.
26. Jones, T.A. FRODO: A graphics fitting program for mac-

romolecules. In: "Computational Crystallography." Sayre, D., ed. Oxford: Clarendon Press, 1982:303–317.
27. Jones, T.A., Thirup, S. A graphics model building and refinement system for macromolecules, using a protein data base of well refined structures. EMBO J. 5:819–822, 1986.
28. Brunger, A.T. XPLOR: Crystallographic refinement by simulated annealing. In: "Crystallographic Computing 4: Techniques and New Technologies." Isaacs, N.W., Taylor, M.R., eds. Oxford: Clarendon Press, 1988:126–140.
29. Moss, D.S., Morffew, A.J. RESTRAIN: Conventional restrained least-squares refinement program. Comput. Chem. 6:1–3, 1982.
30. Haneef, I., Moss, D.S., Stanford, M.J., Borkakoti, N. RESTRAIN: Conventional restrained least-squares refinement program. Acta Crystallogr. A41:426–433, 1985.
31. Cruickshank, D.W.J. Application of weights to structure factor amplitudes. In: "Computing Methods in Crystallography." Rollet, J.S., ed. Oxford: Pergamon Press, 1965: 114–115.
32. Bernstein, F.C., Koetzle, T.F., Williams, G.J.B., Meyer, E.F. Jr, Brice, M.D., Rogers, J.R., Kennard, O., Shimanouchi, T., Tasumi, M. The Protein Data Bank: A computer based archival file for macromolecular structures. J. Mol. Biol. 112:535–542, 1977.
33. Luzatti, V. Treatment of statistical errors in the determination of crystal structures. Acta Crystallogr. 5:802–810, 1952.
34. Ramachandran, G.N., Sasisekaran, V. Representation of the protein male chain conformation. Adv. Protein Chem. 23:283–437, 1968.
35. Lee, B., Richards, F.M. The interpretation of protein structures: Estimation of static accessibility. J. Mol. Biol. 55: 379–400, 1971.
36. Blow, D.M., Janin, J., Sweet, R.M. The crystal structure determination of soybean trypsin inhibitor. Nature (London) 249:52–57, 1974.
37. Sweet, R.M., Wright,H.T., Janin, J., Chothia, C.H., Blow, D.M. The structure determination of soybean trypsin inhibitor complexed with porcine trypsin at 2.6 Å resolution. Biochemistry 13:4212–4228, 1974.
38. Kabsh, W., Sander, C. Dictionary of protein secondary structure: Pattern recognition of hydrogen-bonded and geometrical features. Biopolymers 22:2577–2637, 1983.
39. Richardson, J.S. The anatomy and taxonomy of protein structure. Adv. Protein Chem. 34:167–339, 1981.
40. Sims, J.E., March, C.J., Cosman, D., Widmer, M.B., MacDonald, H.R., McMahan, C.J., Grubin, C.E., Wignall, J.M., Jackson, J.L., Call, S.M., Friend, Alpert, A.R., Gillis, S., Urdal, D.L., Dower, K. Identification of the three immunoglobulin-like domains in the extra-cellular portion of the IL1-receptor, where IL1 might bind. Science 241:585–589, 1988.
41. Davies, D.R., Sheriff, S., Padlan, E.A. Comparison of the crystallographic structures of antigen-antibody complexes. J. Biol. Chem. 263:10541–10544, 1988.
42. Stanfield, R.L., Fieser, T.M., Lerner, R.A., Wilson, I.A. Three dimensional structure solution of an antibody to a peptide and its complex with the peptide antigen at 2.8 Å resolution. Science 248:712–719, 1990.
43. Antoni, G., Presentini, R., Perin, F., Tagliabue, A., Ghiara, P., Censini, S., Volpini, G., Villa, L., Boraschi, D. Peptide analogues of IL1 and biochemical assay of their binding to its receptors. J. Immunol. 137:3201–3204, 1986.
44. Palaszynski, E. Peptide analogues of IL1 and biochemical assay of their binding. Biochem. Biophys. Res. Commun. 147:204–211, 1987.
45. Herzberg, O., Moult, J. Analysis of the steric strain in the polypeptide backbone of protein molecules: Identification of residues in the active site region with abnormal ϕ and ψ using well defined high resolution structures. Proteins 1991, in press.
46. McDonald, H.R., Wingfield, P., Schmeissner, U., Shaw, A., Clore, G.M., Gronenborn, A.M. Different point mutations of IL1-β and analysis of their receptor binding affinity. FEBS Lett. 209:295–298, 1986.
47. Gronenborn, A.M., Clore, G.M., Schmeissner, U., Wingfield, P. Sequence specific assignment of aromatic residues using site-directed mutations in IL1-β. Eur. J. Biochem. 161:37–43, 1986.
48. Huang, J.J., Newton, R.C., Horuk, R., Matthew, J.B., Covington, M., Pezzella, K., Lin, Y. Site-directed mutations in the amino-terminal region of IL1-β and studies on them by circular dichroism spectroscopy. FEBS Lett. 223:294–298, 1987.
49. Horuk, R., Huang, J.J., Covington, M., Newton, R.C. Site-directed mutations in the amino-terminal region of IL1-β and biochemical and kinetic studies of its binding to IL1-receptors. J. Biol. Chem. 262:16275–16278, 1987.
50. Kamogashira, T., Masui, Y., Ohmoto, Y., Hirato, T., Nagamura, K., Mizuno, K., Hong, Y.-M., Kikumoto, Y., Nakai, S., Hirai, Y. Site-specific mutations of cysteine residues in IL1-β. Biochem. Biophys. Res. Commun. 150:1106–1114, 1988.
51. Wingfield, P., Graber, P., Shaw, A.R., Gronenborn, A.M., Clore, G.M., MacDonald, H.R. Site-specific mutations of lysine to cysteine residues in IL1-β. Eur. J. Biochem. 165: 565–571, 1989.
52. Gehrke, L., Jobling, S.A., McDonald, B., Rosenwasser, L.J., Auron, P.E. Point mutations at R12G and analysis of its biological activity by equilibrium receptor binding analysis. J. Biol. Chem. 265:5922–5925, 1990.
53. Veerapandian, B., Gilliland, L.G., Poulos, T.L. Crystallographic structure solution of interleukin-1 β mutants. Manuscript in preparation.
54. Nencioni, L., Villa, L., Tagliabue, A., Antoni, G., Presentini, R., Perin, F., Silvestri, S., Boraschi, D. Peptide analogues of IL1 and their immunostimulatory activity. J. Immunol. 139:800–804, 1987.
55. DeChiara, T.M., Young, D., Semionow, R., Stern, A.S., Batula Bernard, C., Fiedler-Nagy, C., Kaffka, K.L., Kilian, P.L., Yamazaki, S., Mizel, S.B., Lomedico, P.T. Peptide analogues of IL1 and their immunostimulatory activity. Proc. Natl. Acad. Sci. U.S.A. 83:8303–8307, 1986.
56. Mosley, B., Dower, S.K., Gillis, S., Cosman, D. Peptide analogues of IL1 and their immunostimulatory activity. Proc. Natl. Acad. Sci. U.S.A. 84:4572–4576, 1987.
57. Mosley, B., Urdal, D.L., Prickett, K.S., Larsen, A., Cosman, D., Conlon, P.J., Gillis, S., Dower, S.K. Peptide analogues of IL1 and their IL1 activity. J. Biol. Chem. 262: 2941–2944, 1987.
58. Lillquist, J.S., Simon, P.L., Summers, M., Jonak, Z., Young, P.R. Peptide analogues of IL1 and biological activity. J. Immunol. 141:1975–1981, 1988.
59. Jobling, S.A., Auron, P.E., Gurka, G., Webb, A.C., McDonald, B., Rosenwasser, L.J., Gehrke, L. Peptide analogues of IL1 and their biological activity. J. Biol. Chem. 263: 16372–16378, 1988.
60. Rosenwasser, L.J., Webb, A.C., Clark, B.D., Irie, S., Chang, L., Dinarello, C.A., Gehrke, L., Wolff, S.M., Rich, A., Auron, P.E. Peptide analogues of IL1 and their biological activity assay. Proc. Natl. Acad. Sci. U.S.A. 83:5243–5246, 1986.